

OPTICAL AND ELECTRICAL PROPERTIES OF TIN

A. I. GOLOVASHKIN and G. P. MOTULEVICH

P. N. Lebedev Physics Institute, Academy of Sciences, U.S.S.R.

Submitted to JETP editor July 19, 1963

J. Exptl. Theoret. Phys. (U.S.S.R.) **46**, 460-470 (February, 1964)

The following properties of tin were measured: 1) the complex refractive index in the spectral region $0.73-12\mu$ at $T = 293^\circ\text{K}$, and in the region $0.73-11\mu$ at $T = 78^\circ\text{K}$; 2) the static conductivity and its temperature dependence in the range $4.2-293^\circ\text{K}$; 3) the density; 4) the Hall field; 5) the superconducting properties. The data were analyzed taking into account the nature of the skin effect. The conduction electron density, the electron velocity on the Fermi surface, the electron collision frequency, and the Debye temperature of tin were found.

THE present work is a continuation of the study of polyvalent metals, which is being undertaken in the Optics Laboratory of the Physics Institute, U.S.S.R. Academy of Sciences. We carried out a simultaneous study of the optical, electrical and several other properties of white tin, evaporated in vacuum on to a glass substrate. It is essential to investigate simultaneously several properties because during evaporation one may obtain layers with properties differing considerably from those of the bulk metal. Only such a study allows us to determine a number of microproperties of the layers and gives us an idea how close these properties are to those of the bulk metal.^[1]

By special selection of the conditions and the method of evaporation, we obtained tin layers with all their properties close to, or identical with, those of the bulk metal. Therefore, the microproperties determined in the present work can be regarded as representing the bulk metal.

EXPERIMENTAL METHODS

1. To determine the optical constants, we used the polarization method, based on the determination of the phase shift Δ between the p- and s-components of the reflected light and of the azimuth ρ . We used both the phase shifts $\Delta = (\pi/2)(2k+1)$, as well as $\Delta = \pi(2k+1)$, where $k = 0, 1, 2, \dots$ ^[2,3] The measurements were carried out using two setups. The description of one apparatus, which was used to measure the optical constants at room temperature only, was given in^[2]. With this apparatus, at a fixed wavelength of light λ , we measured the angle of incidence φ and the azimuth ρ which characterized the circular polarization of the reflected light. We used quadruple

reflection, and therefore for each wavelength we could find four pairs of values of φ and ρ , corresponding to the phase shifts $\pi/2, 3\pi/2, 5\pi/2$, and $7\pi/2$. The optical constants determined for the same λ but different values of φ were identical. This apparatus allowed us to determine quickly (2-3 hours) the optical constants of the mirrors, prepared in the same evaporation run, over the whole investigated range of wavelengths.

The second apparatus, which was used for measurements both at low temperature and at room temperature, was a modification of that described in^[4]. A parallel beam of light passed first through a rotating polarizer (the frequency of rotation was 4.5 cps), then suffered octuple reflection from the investigated mirrors, passed through an analyzer, was focused on to the slit of a monochromator and finally fell on a bolometer. The bolometer signal was amplified with a resonance amplifier. Both variants of measurements allow us to determine the optical constants in the same way.^[5] Their equivalence follows from the principle of reversibility of light beams.

To make sure that there were no unforeseen additional sources of error, we measured the optical constants of the same mirrors by the two methods. Agreement between the results was very good. The variant used in the present work had the advantage of the absence of a parasitic signal due to the polarization of room radiation by the investigated mirrors; moreover, there was no need to introduce corrections for the polarization of light by the monochromator. The measurements were carried out at a fixed value of the angle of incidence φ . We measured the wavelength λ and the azimuth ρ , corresponding to the values $\Delta = (\pi/2) \times (2k+1)$, where $k = 0, 1, 2, \dots$. For one value of

φ , we used 4–5 pairs of values of λ and ρ .

In this apparatus, we also used the linear polarization of the reflected light. For this, we placed a rotating chopper (9 cps) in front of the investigated mirrors. One of the polarizers was placed at an angle of 45° to the angle of incidence of light, the other was used to determine the azimuth of the re-established polarization. In this case, too, we could determine several pairs of values of λ and ρ , corresponding to the linear polarization of light, for each value of the angle of incidence. We employed 2–3 pairs of values. The use of the phase shift $\Delta = (\pi/2)(2k + 1)$ allowed us to carry out measurements at lower angles of incidence and with higher accuracy than the use of $\Delta = \pi(2k + 1)$ for the same value of k .

In the present work, as in all the preceding studies, special attention was paid to the quality of the polarizers. We used eight selenium films oriented at the angle of 67.5° , which resulted—in the apertures we used—in the intensity of the unwanted transverse component of light being less than $1/500$ the intensity of the longitudinal component over a wide range of wavelengths. Therefore, the error connected with the transmission of the second component by the polarizer was less than the other experimental errors.

As the source of light, we used a dc carbon arc. The light was rendered monochromatic by means of spectrometers with NaCl prisms. Germanium bolometers, made by A. A. Shubin, were used as the receivers. The temperature of the mirrors was measured with a thermocouple.

2. The investigated tin layers were prepared by vacuum evaporation from tantalum boats onto polished glass. The evaporation was carried out at pressures of $(5-8) \times 10^{-6}$ mm Hg. During the evaporation, the vacuum in the chamber did not change because of the large volume of the chamber and the high pumping speed (500 l/min). The purity of the initial tin was greater than 99.99%. The evaporation conditions were selected in a special way. Several trials allowed us to find the conditions which ensured the preparation of thick layers ($0.5-1.1 \mu$) with properties identical with, or close to those of the bulk metal. In this way, very good mirrors without any sign of matt surfaces were obtained. The annealing of the mirrors, carried out at $150-200^\circ\text{C}$ for several hours in vacuum, had no effect on the results of the measurements. Obviously, the quality of our mirrors was much higher than that of the mirrors used by Hodgson,^[6] who investigated either mirrors with a matt deposit or thin transparent mirrors. It is not clear how far the properties of Hodgson's mirrors repre-

sented the properties of the bulk metal.

3. To determine the conductivity, the density, and the Hall effect, special samples were deposited simultaneously with the mirrors. As substrates, we used polished glass plates with fused-in metal leads. The thickness of all these layers was measured by an interference method. To determine the density, the samples were weighed by a microbalance. The resistance was measured in the usual way.

The conductivity of the investigated layers was measured at room temperature, the boiling point of nitrogen, the boiling point of hydrogen, and at helium temperatures. The temperature of the transition to the superconducting state was determined from the resistance discontinuity when the temperature was varied in the absence of a magnetic field. For this purpose, we used the same samples as in the measurements of the conductivity. As usual, the temperature of the superconducting transition was taken to be the temperature at which the resistance of the sample was half the resistance before the transition.

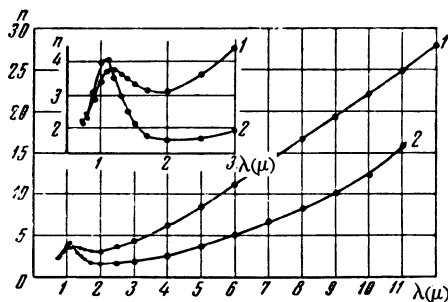
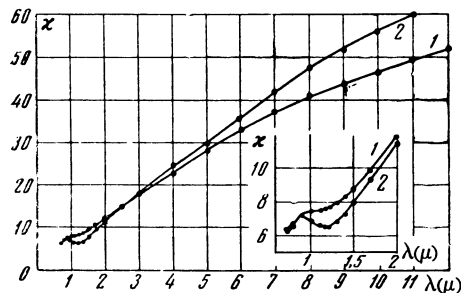
The Hall effect was measured in a constant magnetic field of up to 7 kOe intensity. The Hall emf was determined with a dc amplifier of 10^{-9} V/mm sensitivity. The current densities through the samples were between 100 and 4500 A/cm^2 . The samples used were in the form of strips of deposited tin, 60 mm long, 4 mm wide, and $0.5-1.1 \mu$ thick. The leads for the measurement of the Hall emf were placed at distances of 30 mm from the current leads. Special measures were also taken to ensure that the potential leads were as close as possible to the equipotential location. The remaining small parasitic voltage drop was compensated. The sign of the magnetic field was altered during the measurements, so that we measured a quantity equal to double the Hall emf. Because of the smallness of the Hall emf in tin, special attention had to be paid to careful thermostating of the whole apparatus.

EXPERIMENTAL RESULTS

The experimentally measured values of n and κ are given in Table I and in Figs. 1 and 2 [($n - i\kappa$) is the complex refractive index]. The figures show that at short wavelengths the optical constants are affected by the internal photoeffect. An estimate of the influence of this effect is given below. Here, we can mention only that for $\lambda > 2.5 \mu$ the influence of the internal photoeffect is negligibly small, and we may assume that the optical constants are governed by the conduction electrons.

Table I. Optical constants of tin

λ, μ	$T = 293^\circ \text{K}$		$T = 78^\circ \text{K}$		λ, μ	$T = 293^\circ \text{K}$		$T = 78^\circ \text{K}$	
	n	κ	n	κ		n	κ	n	κ
0.73	2.16	6.35	2.22	6.25	2.5	3.62	14.8	1.69	14.6
0.8	2.38	6.68	2.25	6.48	3.0	4.40	17.8	1.88	18.0
0.9	2.94	7.28	3.04	7.28	4.0	6.18	23.2	2.46	24.2
1.0	3.46	7.40	3.97	6.94	5.0	8.49	28.5	3.75	29.7
1.1	3.68	7.50	4.05	6.60	6.0	11.0	33.1	4.97	35.5
1.15	3.75	7.58	3.81	6.53	7.0	13.8	37.1	6.51	41.4
1.2	3.74	7.68	3.50	6.51	8.0	16.6	40.6	8.17	47.0
1.3	3.65	7.92	2.98	6.79	9.0	19.3	43.8	10.0	51.7
1.4	3.46	8.26	2.48	7.36	10	22.0	46.4	12.4	55.7
1.5	3.29	8.72	2.08	8.04	11	24.8	49.0	15.7	59.8
1.7	3.12	9.92	1.74	9.34	12	27.8	51.6	—	—
2.0	3.09	11.8	1.64	11.4					

FIG. 1. Dependence of the refractive index on λ : 1) $T = 293^\circ \text{K}$; 2) $T = 78^\circ \text{K}$.FIG. 2. Dependence of the absorption index on λ : 1) $T = 293^\circ \text{K}$; 2) $T = 78^\circ \text{K}$.

To determine the optical constants, we carried out many series of measurements using both setups. The measurements with the two setups gave identical results. The error in the determination of n amounted to (1–2)%, and the error in κ was (0.5–1)%. The error was found from the scatter of the values obtained for samples from different evaporation runs. The error in each series of measurements was even smaller. The values of n and κ were determined using the formulas*

$$n = \frac{\sin \varphi \operatorname{tg} \varphi \cos 2\rho'}{1 - \sin 2\rho' \cos \Delta'}, \quad \kappa = \frac{\sin \varphi \operatorname{tg} \varphi \sin 2\rho' \sin \Delta'}{1 - \sin 2\rho' \cos \Delta'},$$

where Δ' and ρ' are the phase shift and the azi-

* $\operatorname{tg} = \tan$.

muth for a single reflection. These formulas do not allow for the dependence of the surface impedance on the angle of incidence φ . Such an allowance leads to a small increase of n and a small reduction of κ . The maximum correction in the 0.7μ region reached 1%; in the 2μ region, it was less than 0.3% and decreased strongly at longer wavelengths. Obviously, there is no sense in introducing such a small correction.

In one apparatus, the light incident on the mirrors had a narrow spectral range (after passing through a monochromator), while in the other apparatus, the light encompassed a very wide range of wavelengths ($\lambda \gtrsim 0.7 \mu$). The agreement between the experimental results obtained in these two ways indicated the absence of the influence on the optical constants of the additional illumination with short-wavelength radiation (such an effect is observed only in semiconductors). The absence of this effect in the second apparatus was also specially checked by means of filters which cut off the short-wavelength radiation.

The measurements of the optical constants were carried out both immediately after the preparation of the mirrors, and after one day in vacuum. The results were the same. We also carried out a special investigation of the influence of a 48-hour exposure of the mirrors to the atmosphere. The change in the optical constants produced by this exposure was less than (2–3)% in the case of n and less than 1% in the case of κ . All the measurements of the optical constants were carried out during much shorter intervals of time (of the order of several hours).

The optical constants of tin at room temperature have been determined by Motulevich and Shubin^[2], as well as by Hodgson.^[6] The results reported in^[2] refer only to the spectral range 1.3–6.3 μ , within which they agree well with the results of the present work. Hodgson^[6] gave his results only in

Table II. Electrical and some other properties of tin

	Investigated layers	Bulk metal		Investigated layers	Bulk metal
d, μ	0.5—1.1		R_{res}/R_0	$3.5 \cdot 10^{-2}$	10^{-3}
$\rho, \text{g/cm}^3$	7.2	7.28	$T_{\text{cr}}, \text{°K}$	3.88	3.73
$\sigma_0, \text{cgs esu}$	$7.1 \cdot 10^{16}$	$7.8 \cdot 10^{16}$	$\Delta T, \text{°K}$	0.01—0.03	0.01
$\sigma_{\text{N}}, \text{cgs esu}$	$3.1 \cdot 10^{17}$	$4.0 \cdot 10^{17}$	$E_x/j (\mu\Omega \times \text{cm in}$	$\pm 5.0 \cdot 10^{-3}$	$-4.1 \cdot 10^{-3}$
$\sigma_{\text{H}}, \text{cgs esu}$	$1.5 \cdot 10^{18}$	$6.7 \cdot 10^{18}$	$H = 1 \text{ kOe})$		

the form of a graph of the dependences of $\log(\kappa^2 - n^2 + 1)$ and $\log(n\kappa/\lambda)$ on $\log \lambda$. All the results were obtained on a single layer. The values of n and κ could be found from Hodgson's data only very roughly so that we could note only a qualitative agreement between the nature of the dependences of n and κ on λ . The electrical and other properties of the investigated layers were not reported in [2] or [6].

The experimentally determined electrical and other parameters of our tin layers are given in Table II. The same table also includes the values of these parameters for the bulk metal. The first line gives the thickness of the investigated layers. As mentioned above, the investigated parameters were found to be independent of the thickness in the case of our layers. Thinner layers did exhibit such a dependence (all the data in Tables I and II refer to "thick" layers). The density ρ was measured with an accuracy of 5%. It is seen that the density of the layers was identical with the bulk metal density.

The conductivity was measured with an accuracy of 5%.¹⁾ The conductivity at room temperature, σ_0 (given in the third line of Table II), was measured at $T = 293^\circ\text{K}$; its value was 91% of the bulk metal conductivity. The conductivity at the temperature of liquid nitrogen, σ_{N} (given in the fourth line), refers to $T = 77.4^\circ\text{K}$; it amounted to 78% of the bulk metal conductivity. The conductivity at room and nitrogen temperatures was independent of the thickness, even in the case of layers $\approx 0.2 \mu$ thick. The fifth line of Table II gives the conductivity at the temperature of liquid hydrogen, σ_{H} (it refers to $T = 20.3^\circ\text{K}$). The latter quantity amounted to 22% of the bulk metal conductivity.²⁾ The sixth line in Table II (the first line in the right-hand

half) gives the ratio of the residual resistance R_{res} to the resistance at room temperature R_0 . The residual resistance was determined at liquid helium temperatures. It did not vary between $T = 4.2^\circ\text{K}$ and the temperature of the superconducting transition. With a reduction in the thickness, the residual resistance increased somewhat. The difference between the values of R_{res}/R_0 and $[1 - (\sigma_0/\sigma_{\text{b}})]$, where σ_{b} is the bulk metal conductivity at $T = 293^\circ\text{K}$, was due to the somewhat lower Debye temperature of our samples compared with the Debye temperature of bulk tin. The determination of the Debye temperature is described below.

The next two lines in Table II give the temperature of the transition to the superconducting state T_{cr} and the temperature range in which this transition occurs. The value of T_{cr} was close to that of the bulk metal. The transition in the layers was very sharp, indicating their good uniformity.

The last line in Table II gives the ratio of the Hall field and the current density through a sample in a magnetic field $H = 1 \text{ kOe}$. This ratio was determined with an accuracy of 30%. It was independent of the current density. We determined the dependence of the Hall field on the magnetic field. Up to $H = 7 \text{ kOe}$, the Hall field was proportional to the magnetic field. Table II shows that the value of the Hall effect in the test samples was very small, as in the case of bulk tin (30 times smaller than in the case of copper or gold). This represents an almost complete compensation of the electron Hall effects by the "hole" effect. The test samples showed a slight dominance of the influence of "holes" while a bulk polycrystal showed a slight dominance of electrons. In tin single crystals, the sign of the effect is different for different directions but the value of the effect remains small.^[8] In all cases, the Hall effect was practically equal to zero.

¹⁾The accuracy of the determination of both the density and the conductivity was governed by the accuracy of the thickness measurement.

²⁾The bulk-metal conductivities, taken from various handbooks, differ by 20-30%.^[7] Table II lists the most reliable values.

ANALYSIS OF THE EXPERIMENTAL DATA

The analysis of the optical experimental data was carried out taking into account the skin effect,

which was found to be weakly anomalous both at room temperature and at liquid nitrogen temperature.

The conduction electron density N , the velocity of electrons on the Fermi surface v , and the frequency of electron collisions ν_{opt} , were determined using the following formulas:^[9]

$$N = \frac{0.1115 \cdot 10^{22} (n^2 + \kappa^2)^2}{\lambda^2 \kappa^2 - n^2} (1 + \beta_1), \quad (1)$$

$$\frac{\nu_{\text{opt}}}{N} = 1.690 \cdot 10^{-6} \lambda \frac{2n\kappa}{(n^2 + \kappa^2)^2} (1 - \beta_2), \quad (2)$$

$$\beta_1 = \text{Re } \gamma + \frac{2n\kappa}{\kappa^2 - n^2} \text{Im } \gamma, \quad (3)$$

$$\beta_2 = \text{Re } \gamma - \frac{\kappa^2 - n^2}{2n\kappa} \text{Im } \gamma, \quad (4)$$

$$\gamma = \frac{3}{8} \frac{v}{c} \kappa \frac{\sqrt{1 + n^2 \kappa^2}}{\sqrt{1 + \nu_{\text{opt}}^2 / \omega^2}} \exp [i(\varphi_1 - \varphi_2)], \quad (5)$$

where $\tan \varphi_1 = n/\kappa$, $\tan \varphi_2 = \omega/\nu_{\text{opt}}$. Here, ω is the angular frequency of light, λ is the wavelength of light in microns, and c is the velocity of light in vacuum. The calculations were carried out by the method of successive approximations. In the zeroth approximation, we assumed that $\beta_1 = \beta_2 = 0$. This corresponds to the normal skin effect. For each λ , we determined $N^{(0)}$ in the zeroth approximation; this value showed some dependence on λ . The average value of $N^{(0)}$ was used to determine $\nu_{\text{opt}}^{(0)}$ in the zeroth approximation using Eq. (2). In principle, $\nu_{\text{opt}}^{(0)}$ could depend on the frequency and therefore, in determining the corrections β_1 and β_2 , we used the value of $\nu_{\text{opt}}^{(0)}$ determined for a given frequency.

The value of β_1 was determined using Eq. (3). The unknown parameter v was selected so that the right-hand part of Eq. (1) was independent of λ . In order to find v easily and reliably, we used the least squares method. Since in the case of tin the skin effect is weakly anomalous, the magnitude of the correction β_1 is small, which appears as a weak dependence of $N^{(0)}$ on λ . Therefore, for a reasonably reliable determination of v , the optical constants must be measured accurately. The accuracy of our optical measurements gave v with an error of 15%. This value of v was used to find the correction β_2 . Next, using Eqs. (1) and (2), we found N and ν_{opt} in the first approximation. The second approximation gave values practically identical with those in the first approximation.

To determine the microproperties related to free electrons, we used the wavelength range 2.5–12 μ . At shorter wavelengths, the optical constants were considerably affected by the internal photoeffect. The determination of the absorption coefficient for normal incidence $A = 4n/[(n+1) + \kappa^2]$

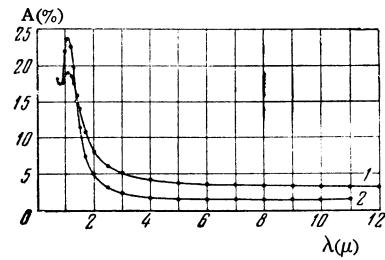


FIG. 3. Dependence of the absorption coefficient. $A = 4n/[(n+1) + \kappa^2]$ on λ : 1) $T = 293^\circ\text{K}$; 2) $T = 78^\circ\text{K}$.

indicated the presence of a sharp peak in the 1–1.2 μ region (cf. Fig. 3).

Tin belongs to the fourth group in the periodic table and has four valence electrons per atom: two s-electrons and two p-electrons. Obviously, the p-electrons are on the Fermi surface and the internal photoeffect is due to the transfer of the s-electrons to the Fermi level. We attempted to estimate the influence of the internal photoeffect. Assuming that the complex permittivities, related to free electrons and electrons taking part in the internal photoeffect, are additive, we can determine the real and imaginary components of the permittivity, due to free electrons, over the whole range of wavelengths using the dependences $n(\lambda)$ and $\kappa(\lambda)$ at the long-wavelength end. Subtracting the electronic component from the experimentally measured complex permittivity, we can obtain the contribution of the internal photoeffect. It was found that the wavelength dependence of the permittivity component related to the internal photoeffect was of the dispersion type. A more detailed consideration of the problem of the influence of the internal photoeffect will be given in a separate communication. We would point out only that in the case of tin is the experimentally determined wavelength dependence of the permittivity related to the internal photoeffect steeper than the dispersion curve but flatter than an exponential curve. The internal photoeffect contribution, determined even from the steeper dispersion formulas, was found to be negligibly small already at $\lambda = 2\text{--}3 \mu$.

Before giving the final results of our analysis of the experimental data, we shall describe how we found the Debye temperature for our samples. We started from the assumption that the reduced resistance of tin is $r = 1.056 (T/\Theta) F(\Theta/T)$, where $F(\Theta/T)$ is the function tabulated in ^[10,11], and Θ is the Debye temperature. We had to find the value of Θ for the temperature range 78–293°K; for this, we used the relationship

$$\frac{R_N - R_{\text{res}}}{R_0 - R_{\text{res}}} = \frac{T_N F(\Theta/T_N)}{T_0 F(\Theta/T_0)}.$$

Table III. Microproperties of tin

	$T=293^\circ\text{K}$	$T=78^\circ\text{K}$		$T=293^\circ\text{K}$	$T=78^\circ\text{K}$
N, cm^{-3}	$4.8 \cdot 10^{22}$	$4.2 \cdot 10^{22}$	β_1	$\lambda = 2,5 \mu$	0.005
N/N_a	1.3	1.1		$\lambda = 11 \mu$	0.03
$v, \text{cm/sec}$	$0.93 \cdot 10^8$	$1.0 \cdot 10^8$	β_2	$\lambda = 2,5 \mu$	0.04
$v_{\text{opt}}, \text{sec}^{-1}$	$2.26 \cdot 10^{14}$	$0.76 \cdot 10^{14}$		$\lambda = 11 \mu$	0.045
$v_{\text{cl}}^{\text{ef}}, \text{sec}^{-1}$	$1.64 \cdot 10^{14}$	$0.28 \cdot 10^{14}$		max β_2	0.055
$v_{\text{cl}}^{\text{ed}}, \text{sec}^{-1}$	$6 \cdot 10^{12}$	$6 \cdot 10^{12}$		l, cm	$0.4 \cdot 10^{-6}$
$v_{\text{eff}}, \text{sec}^{-1}$	$1.70 \cdot 10^{14}$	$0.56 \cdot 10^{14}$		δ, cm	$2.8 \cdot 10^{-6}$

Here, R_0 , R_N , and R_{res} are the resistances at 293°K , 77.4°K , and 4.2°K , respectively; T_0 and T_N are the room temperature and the boiling point of nitrogen, respectively. There was no difficulty in determining Θ from this relationship. The value of Θ found for a large number of samples was $187 \pm 3^\circ\text{K}$. The same method of determining Θ , applied to the bulk metal, gave values of Θ between 193 and 208°K . This scatter of the Debye temperatures is due to the fact that different handbooks give different temperature dependences to the resistance of tin.^[3] The average value of the Debye temperature determined from the specific heat is $\Theta = 189^\circ\text{K}$.^[11] Taking into account this scatter of the Debye temperature values, obtained by different authors, we may assume that the Debye temperature of our samples is close to the Debye temperature of bulk tin. Later, we shall use our Debye temperature to determine the effective electron collision frequency.

The results of the analysis of the experimental data are listed in Table III. The first line gives the average value of the conduction electron density. The results of the determinations of this density for various wavelengths are given in Fig. 4, which shows clearly its remarkable constancy in the $2-11 \mu$ region. It was found that the conduction electron densities in tin at $T = 293^\circ\text{K}$ and $T = 78^\circ\text{K}$ differ by an amount which is considerably greater than the experimental error.

In the metals investigated earlier—aluminum, lead, gold, silver, copper^[12-14]—the conduction electron density was found to be independent of temperature, which indicates that the band structure did not vary with temperature. The variation of the electron density in tin is obviously due to changes in the band structure on cooling. Tin has four valence electrons per atom and crystallizes in a deformed diamond lattice. Elements of the fourth group with the diamond lattice—germanium, silicon, and α -tin—are semiconductors. The metallic properties of tin are due to the overlap of

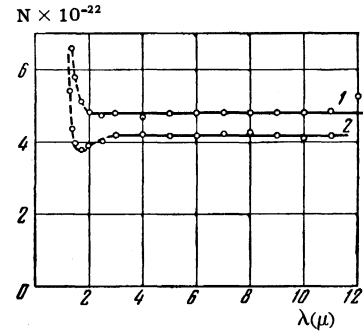


FIG. 4. Dependence, on λ , of the quantity $N = \frac{0.1115 \times 10^{22}(n^2 + \kappa^2)^2}{\lambda^2(\kappa^2 - n^2)} (1 + \beta_1)$ (in the $2.5 - 11 \mu$ region, this quantity gives the conduction electron density): 1) $T = 293^\circ\text{K}$; 2) $T = 78^\circ\text{K}$.

the energy bands. Obviously, this overlap varies with temperature.

The second line in Table III gives the ratio of the conduction electron density to the concentration of atoms (N_a). A determination of this quantity from the surface impedance in the radio-frequency range at helium temperatures gave an average value $N/N_a = 1.2$.^[11] This is in good agreement with our value at $T = 78^\circ\text{K}$.

When the value of N is determined optically, it is not necessary to divide the Fermi surface into an electron part and a hole part. This can be seen even from the fact that $\epsilon \sim e^2$. However, if such a division is effected, it is necessary to assume that the optical measurements give the quantity $N/m = N^e/m_{\text{eff}}^e + N^h/m_{\text{eff}}^h$, where N^e and N^h are the electron and hole densities, m is the free-electron mass, m_{eff}^e and m_{eff}^h are the effective masses of electrons and holes. In the case of the Hall effect, such a separation is important; the total effect is determined by the difference of the electron and hole effects. The Hall field value given in Table II, both for the investigated tin layers and for the bulk metal, is extremely small (30 times smaller than the Hall field of copper), which indicates that the electron and hole contri-

butions practically balance each other out. The whole effect is due to the small difference between the electron and hole mobilities.

The third line of Table III gives the electron velocity on the Fermi surface. As pointed out above, this quantity was determined with an error of 15%, and therefore the values obtained for 293 and 78°K can be regarded as identical. The value of the electron velocity on the Fermi surface obtained from the optical measurements agrees with the value obtained from the measurements of the electronic specific heat of tin. Using our value of N at $T = 78^\circ\text{K}$ and the data of Eisenstein,^[15] we find that $v = 0.92 \times 10^8$ cm/sec, which agrees with our data.

The fourth line of Table III gives the electron collision frequency, ν_{opt} , found from the optical data at the long-wavelength end of the spectral range. The dependence of this quantity on λ is given in Fig. 5. This figure shows that it is not possible to separate out the quadratic dependence related to the collisions between electrons. This is because in the case of tin, due to the internal photoeffect, we cannot use the short-wavelength part of the spectrum where the influence of the electron-electron collisions is greatest. In the long-wavelength region, the influence of the electron-electron collisions is extremely small compared with the strong electron-phonon interaction.

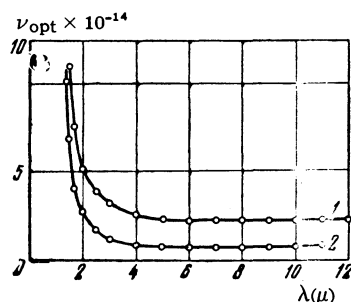


FIG. 5. Dependence of the electron collision frequency on λ : 1) $T = 293^\circ\text{K}$; 2) $T = 78^\circ\text{K}$.

The values obtained for the conduction electron density and the static values of the conductivity of the investigated layers at various temperatures (cf. Table II) can be used to determine the classical electron-phonon collision frequency, $\nu_{\text{cl}}^{\text{ep}}$, and the frequency of collisions of electrons with impurities or defects, ν^{ed} .^[13] The values of these quantities at both temperatures are listed in lines 5 and 6 of Table III. We should remember that in the presence of light the interaction between electrons and phonons involves quantum effects calculated by Gurzhi.^[16] According to Gurzhi, we can

calculate the effective electron collision frequency, $\nu_{\text{eff}} = \nu^{\text{ed}} + \nu_{\text{cl}}^{\text{ep}} \varphi(T/\Theta)$, where $\varphi(T/\Theta)$ is a function calculated by Gurzhi. The value determined in this way is given in line 7 of Table III. One would expect ν_{eff} to coincide with ν_{opt} , but it was found that $\nu_{\text{opt}} > \nu_{\text{eff}}$ at both temperatures.

This difference is possibly due to the inaccuracy in the determination of $\varphi(T/\Theta)$. In Gurzhi's work, this function was found to within a multiplier of the order of 2. It is of interest to check the temperature dependence of $\varphi(T/\Theta)$ predicted by Gurzhi. For this purpose, we shall calculate the ratio $(\nu_{\text{opt}} - \nu^{\text{ed}})/\nu_{\text{cl}}^{\text{ep}}$ at temperatures of 293 and 78°K, and compare it with the corresponding ratio of the values of the function $\varphi(T/\Theta)$ at the same temperatures ($\Theta = 187^\circ$). The former value was 0.54 and the latter 0.57. This agreement can be regarded as quite satisfactory. An accurate check of the temperature dependence requires measurements at lower temperatures.

The rest of Table III gives the values of the correction coefficients β_1 and β_2 , which allow for the role of the effects related to the diffuse nature of the electron reflections from the surface of the metal. The values of these coefficients are given for the two wavelengths indicated in Table III. The table also gives the maximum value of the coefficient β_2 . It is evident that these coefficients are small and that we can use the above formulas, but if these coefficients are neglected considerable errors are introduced. We note that $\beta_2 > \beta_1$, and therefore a correction is much more important in the determination of ν_{opt} than in the determination of N .

The last two lines in the right-hand half of Table III gives the values of the electron mean free path l and the skin-layer depth $\delta = \lambda/2\pi\kappa$. Both these quantities depend weakly on λ ; the values in Table III are given for $\lambda = 5 \mu$. It is seen that $l < \delta$. Although at $T = 293^\circ\text{K}$, the ratio l/δ amounts to $1/7$, all the corrections due to the anomalous nature of the skin effect are still important. At $T = 78^\circ\text{K}$, $l/\delta = 1/2$ and the correction β_2 reaches 16%.

Using the values of v and ν^{ed} , we can estimate the dimensions of crystallites in the investigated layers:

$$L \approx v/\nu^{\text{ed}} \approx 0.15 \mu.$$

Thus, our simultaneous investigation of the optical, electrical and several other properties of tin allowed us to determine a number of microproperties. These properties represented the bulk metal. The results obtained from the optical data were in

good agreement with the results found by other methods. The constancy of N , determined over a wide range of wavelengths, indicated the applicability of our model to polyvalent metals.

The formulas used in the analysis of the experimental data assumed that the Fermi surface was spherical. In the case of polycrystals, we are quite justified in using these formulas. It is then assumed that we obtain some average values of the microproperties. However, it seems to us that the assumption of the Fermi surface sphericity is justified also for tin single crystals. The latest most accurate investigations of the Fermi surface by the cyclotron resonance method carried out by Khaikin,^[17] support Harrison's scheme.^[18] The principal radius of the Harrison sphere was refined by only 2–3%. Departures from the Fermi surface sphericity were found at small regions near the Brillouin zone boundaries, representing small electron groups. The contribution of these electrons to the optical constants can be neglected. It seems to us that the difference between the static conductivities of tin at right-angles and parallel to the fourfold axis ($\sigma_{\perp}/\sigma_{\parallel} = 1.45$) is due to the anisotropy of the elastic properties, leading to a slight dependence of the frequency of the electron-phonon collisions on the direction.³⁾ Therefore, the anisotropy of the quantity ν_{opt} must be allowed for in an investigation of tin single crystals.

¹G. P. Motulevich, JETP 37, 1770 (1959), Soviet Phys. JETP 10, 1249 (1960).

²G. P. Motulevich and A. A. Shubin, Optika i spektroskopiya 2, 633 (1957).

³I. V. Shklyarevskii and V. K. Miloslavskii, Optika i spektroskopiya 3, 361 (1957).

⁴Golovashkin, Motulevich, and Shubin, PTÉ, No. 5, 74 (1960).

⁵G. K. T. Conn and G. K. Eaton, J. Opt. Soc. Amer. 44, 484 (1954).

⁶J. N. Hodgson, Proc. Phys. Soc. (London) B68, 593 (1955).

³⁾An indirect confirmation of this assumption is the fact that, according to the work of Aleksandrov and D'yakov,^[19] the residual resistance of tin single crystals is isotropic.

⁷Ya. G. Dorfman and S. É. Frish (ed.), Sbornik fizicheskikh konstant (Collection of Physical Constants), ONTI, 1937; Handbook of Chemistry and Physics, Cleveland, Ohio, 33rd edition; C. J. Smithells, Metal Reference Book, Butterworths 1955, 2nd edition; W. H. J. Childs, Physical Constants, Methuen, 1949 (Russ. Transl. Fizmatgiz, 1962); G. W. C. Kaye and T. H. Laby, Tables of Physical and Chemical Constants, Longmans, 1959, 12th edition (Russ. Transl., Fizmatgiz, 1962).

⁸V. N. Kachinskiĭ, DAN SSSR 135, 818 (1960), Soviet Phys. Doklady 5, 1260 (1960); JETP 43, 1158 (1962), Soviet Phys. JETP 16, 818 (1963); J. M. Ziman, Electrons and Phonons, Clarendon Press, Oxford, 1960 (Russ. Transl. IIL, 1962).

⁹G. P. Motulevich, JETP 46, 287 (1964), Soviet Phys. JETP (in press).

¹⁰E. Grüneisen, Ann. Physik 16, 530 (1933).

¹¹Low Temperature Physics. Handbuch d. Physik. v. 14–15, Springer, 1956 (Russ. Transl. IIL, 1959).

¹²Golovashkin, Motulevich, and Shubin, JETP 38, 51 (1960), Soviet Phys. JETP 11, 38 (1960).

¹³A. I. Golovashkin and G. P. Motulevich, JETP 44, 398 (1963), Soviet Phys. JETP 17, 271 (1963).

¹⁴V. G. Padalka and I. N. Shklyarevskii, Optika i spektroskopiya 11, 527 (1961); 12, 291 (1962).

¹⁵J. Eisenstein, Revs. Modern Phys. 26, 277 (1954).

¹⁶R. N. Gurzhi, JETP 33, 451, 660 (1957), Soviet Phys. JETP 6, 352, 506 (1958); Dissertation, Physico-technical Institute, Academy of Sciences, U.S.S.R., 1958.

¹⁷M. S. Khaikin, JETP 43, 59 (1962), Soviet Phys. JETP 16, 42 (1963); Dissertation, Institute for Physics Problems, Academy of Sciences, U.S.S.R., 1963.

¹⁸W. A. Harrison, Phys. Rev. 118, 1190 (1960); 116, 555 (1959). A. V. Gold and M. G. Priestley, Phil. Mag. 5, 1089 (1960).

¹⁹B. N. Aleksandrov and I. G. D'yakov, JETP 43, 852 (1962), Soviet Phys. JETP 16, 603 (1963).

Translated by A. Tybulewicz